

Large local disorder in the superconducting $K_{0.8}Fe_{1.6}Se_2$ studied by extended x-ray absorption fine structure

A. Iadecola¹, B. Joseph¹, L. Simonelli², A. Puri³, Y. Mizuguchi^{4,5}, H. Takeya^{4,5}, Y. Takano^{4,5}, N. L. Saini¹

¹Dipartimento di Fisica, Università di Roma “La Sapienza”, P. le Aldo Moro 2, 00185 Roma, Italy

²European Synchrotron Radiation Facility, 6 RUE Jules Horowitz BP 220 38043 Grenoble Cedex 9 France

³INFN -Laboratori Nazionali di Frascati, via E. Fermi 40, 00044 Frascati, Roma, Italy

⁴National Institute for Materials Science, 1-2-1 Sengen, Tsukuba 305-0047, Japan

⁵JST-TRIP, 1-2-1 Sengen, Tsukuba 305-0047, Japan

Abstract.

We have measured local structure of superconducting $K_{0.8}Fe_{1.6}Se_2$ chalcogenide ($T_c=31.8$ K) by temperature dependent polarized extended x-ray absorption fine structure (EXAFS) at the Fe and Se K-edges. We find that the system is characterized by a large local disorder. The Fe-Se and Fe-Fe distances are found to be shorter than the distances measured by diffraction, while the corresponding mean square relative displacements reveal large Fe-site disorder and relatively large c -axis disorder. The local force constant for Fe-Se bondlength ($k\sim 5.8$ eV/Å²) is similar to the one found in the binary FeSe superconductor, however, the Fe-Fe bondlength appears to get flexible ($k\sim 2.1$ eV/Å²) in comparison to the binary FeSe ($k\sim 3.5$ eV/Å²), an indication of partly relaxed Fe-Fe networks in $K_{0.8}Fe_{1.6}Se_2$. The results suggest glassy nature of the title system, with the superconductivity being similar to the one in the granular materials.

Journal reference: Journal of Physics: Condensed Matter 24 (2012) 115701

PACS numbers: 74.70.Xa;74.81-g;61.05.cj;78.70.Dm

1. Introduction

Discovery of superconductivity in the iron-based ‘1111’ pnictides [1] boosted renewal of research activities in the field, resulting a number of iron containing superconductors with different transition temperatures, the maximum being about 55 K for the SmFeAsO system [2, 3]. Among these, the FeSe (the 11-type chalcogenide) shows lowest superconducting transition temperature ($T_c \sim 8$ K), however, could be considered as a model system to address basic characteristics of these materials [3]. The FeSe structure contains simple stacking of tetrahedrally coordinated $FeSe_4$ layers without spacer layers that are known to have substantial effect on the electronic properties [4, 5]. Substitution by Te in the FeSe leads to a marginal increase in the T_c (~ 15 K), however, the system gets phase separated and the nanoscale structure is characterized by different iron-chalcogen bondlengths [8]. On the other hand, the superconducting transition temperature of the FeSe shows large enhancement up to ~ 37 K under the hydrostatic pressure [6, 7]. A large pressure sensitivity of the FeSe indicates chemical pressure being a potential alternative parameter for raising its T_c . Indeed, superconductivity at a T_c as high as 32 K has been observed recently in a K-intercalated FeSe [9], triggering new studies on the iron-based chalcogenides. Later, similar T_c has been observed in the $Rb_xFe_{2-y}Se_2$ [10, 11], $(Tl,K)Fe_{2-y}Se_2$ [12] and $Cs_xFe_{2-y}Se_2$ [13] compounds.

There appears a substantial charge transfer between the active FeSe blocks and the intercalated spacer layers in the $K_xFe_{2-y}Se_2$, with electrons from the K^+ ions filling the hole bands at the zone center. Thus, the Fermi surface of $K_xFe_{2-y}Se_2$ is made by only the electron pockets around the M points [15, 14], and hence the scenario based on the nesting between electron and hole pockets, usually argued to understand the iron pnictides, loses its ground [16]. On the other hand, although isostructural to the 122-type $BaFe_2As_2$ pnictides, the $K_xFe_{2-y}Se_2$ has distinct microstructure, characterized by an iron-vacancy order and a phase separation [17, 18, 19, 20]. The magnetic order with a remarkably large iron magnetic moment co-exists with bulk superconductivity [21, 22]. In addition, there are experimental indications on the relation between the superconductivity and the iron-vacancy disorder, with a completely ordered state being an insulator. These facts point out that a complete knowledge of the nanoscale structure is needed for describing the fundamental electronic structure of these materials.

Extended x-ray absorption fine structure (EXAFS), an atomic site-specific experimental probe [23], has been widely used to study local structure of different materials, including the copper oxide superconductors and related systems [24]. EXAFS has also been exploited to study the new iron-based superconductors, revealing important information on the atomic correlations between different layers [4, 5] and temperature dependent local structural anomalies across the superconducting transition [25, 26]. More recently, we have applied EXAFS to study the local structure of $FeSe_{1-x}Te_x$ chalcogenides, providing direct evidence of phase separation in the ternary systems, characterized by different Fe-Se and Fe-Te distances [8]. In the present study, we have used polarized EXAFS to explore the local structure of $K_{0.8}Fe_{1.6}Se_2$

superconductor. The results of polarized EXAFS at the Fe and Se K-edges reveal large local disorder similar to the amorphous/glass materials. The local structure of $K_{0.8}Fe_{1.6}Se_2$ is significantly different from the local structure of the binary FeSe [8] superconductor. While the local force constant of Fe-Se bondlength ($k \sim 5.8 \text{ eV/\AA}^2$) is similar in the two systems, the one for the Fe-Fe bondlength appears to sustain substantial changes due to K intercalation ($k \sim 3.5 \text{ eV/\AA}^2$ and $k \sim 2.1 \text{ eV/\AA}^2$ respectively for FeSe and $K_{0.8}Fe_{1.6}Se_2$ systems), consistent with a partial relaxation of the Fe-Fe networks due to the K-intercalation. The experimental results suggest that glass physics should have distinct role in the understanding of these superconductors.

2. Experimental Details

X-ray absorption measurements were performed at the beamline BM23 in the European Synchrotron Radiation Facility (ESRF), Grenoble on well characterized single crystal of $K_{0.8}Fe_{1.6}Se_2$ system. The single crystal was grown by melting a precursor of FeSe and K placed in an alumina crucible, that itself was sealed into an arc-welded stainless steel tube. The details on the crystal growth and characterization for superconducting, structural and transport properties are described elsewhere [27]. A platelike and dark-shining as grown single crystal with $T_c = 31.8 \text{ K}$ was selected and detailed synchrotron x-ray diffraction study [17] was performed prior to the x-ray absorption measurements. The synchrotron radiation emitted by a bending magnet source at 6 GeV ESRF storage ring was monochromatized by a double crystal Si(311) monochromator. The polarized EXAFS measurements at the Fe and Se K-edges were acquired in the normal incidence (with polarization parallel to the ab-plane and hereafter called $E \parallel ab$ polarization) and in the grazing incidence geometry (10 degree off the $E \parallel c$ and hereafter called $E \parallel c$ polarization). Fluorescence mode was used (exploiting a multi-element Ge-detector system) for the measurements. The samples were mounted in a continuous flow He cryostat and the temperature was controlled and monitored within an accuracy of $\pm 1 \text{ K}$. Several spectral scans were acquired at each temperature to ensure the reproducibility of the measurements. Standard procedure was used to extract the EXAFS signal from the absorption spectrum [23] and corrected for the fluorescence self-absorption before the analysis [28].

3. Results and Discussion

Figure 1 shows Fourier transform (FT) magnitudes of the polarized EXAFS oscillations, measured at the Se and Fe K-edges on $K_{0.8}Fe_{1.6}Se_2$ single crystal. The FT magnitudes provide partial atomic distribution around the Se and Fe in the direction of x-ray beam polarizations. Se K-edge EXAFS, measured in the $E \parallel ab$ polarization shows only the contribution from the nearest neighbour Fe atoms at a distance $\sim 2.4 \text{ \AA}$ (main peak in the FT at $\sim 2 \text{ \AA}$). The next nearest neighbours of Se in the $E \parallel ab$ geometry are K ($R = 3.45 \text{ \AA}$), Se ($R = 3.91$ and 4.02 \AA) and Fe ($R = 4.62 \text{ \AA}$) atoms, and their contributions

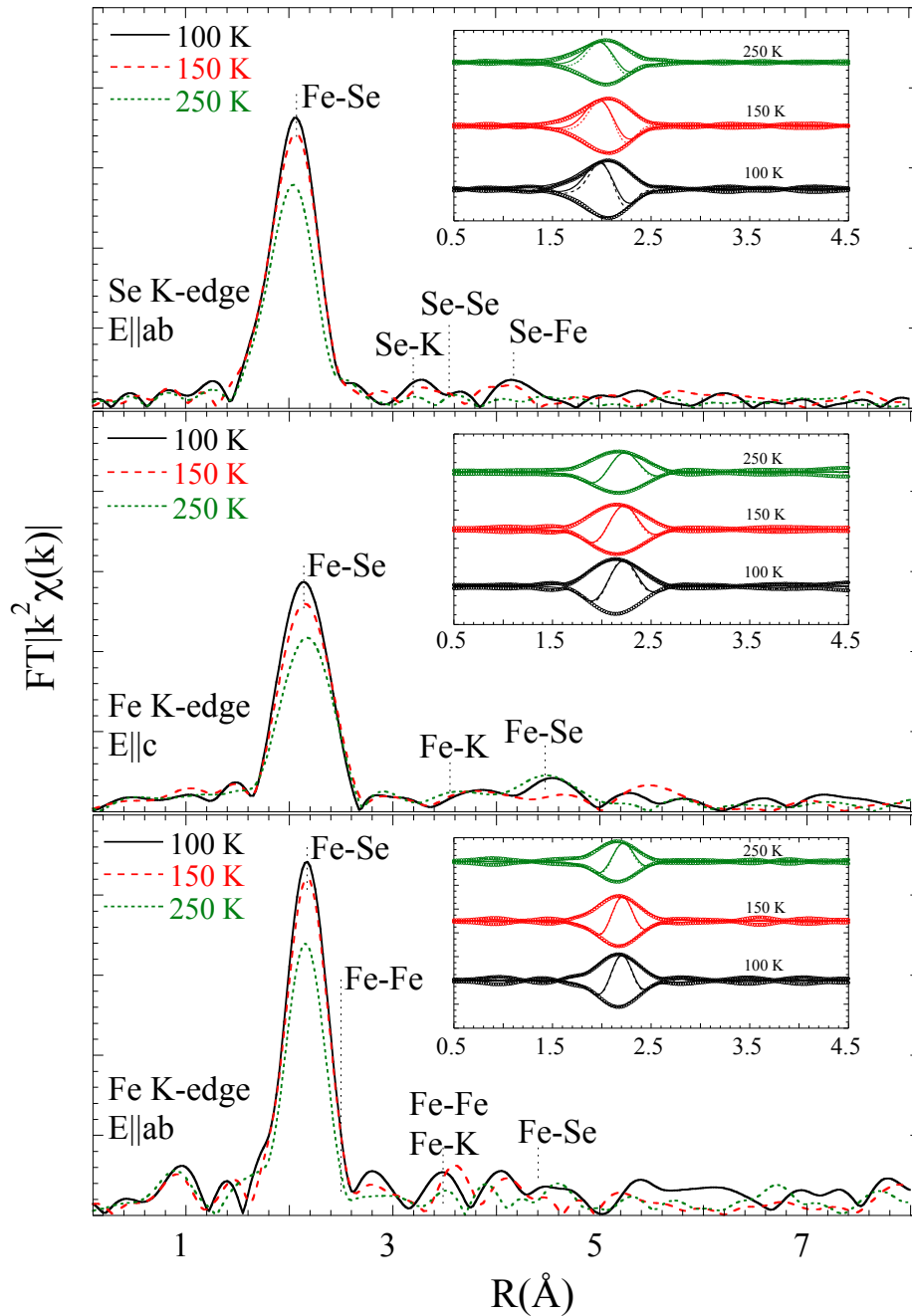


Figure 1. Fourier transform (FT) magnitudes of the polarized EXAFS (weighted by k^2) measured on $K_{0.8}Fe_{1.6}Se_2$ single crystal at several temperatures. The measurements were made at Se K-edge in the $E||ab$ (upper) polarization and, at Fe K-edge in the $E||ab$ (lower) and $E||c$ (middle) polarizations. The FT are performed using a Gaussian window and not corrected for the phase shifts. The k -range is 3.5 - 15.5 \AA^{-1} for the $E||ab$ EXAFS, and 3.5 - 14 \AA^{-1} for the $E||c$ data. The insets show experimental FT magnitudes and real parts with the model fits (solid lines).

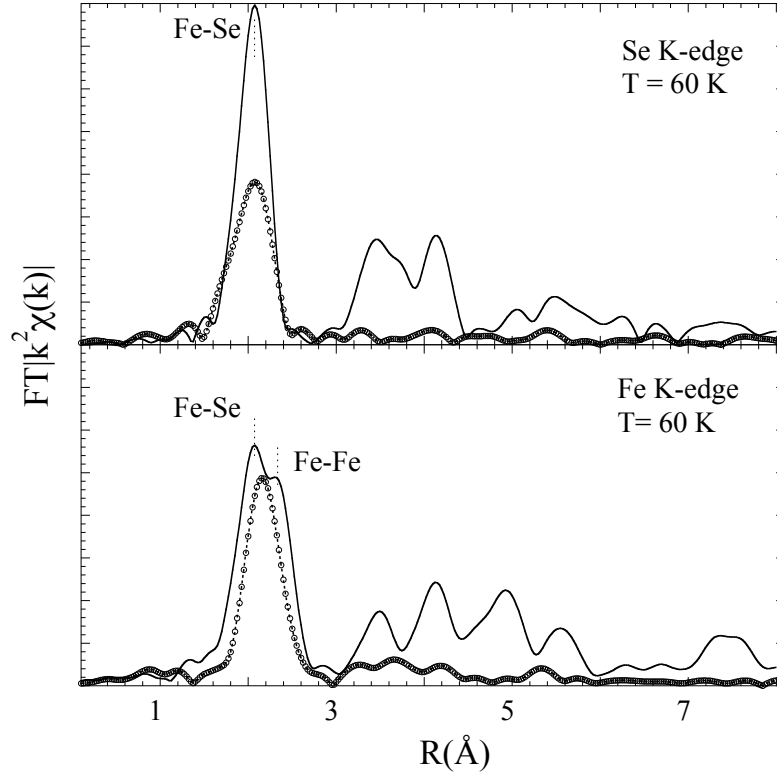


Figure 2. Fourier transform magnitudes of the Fe K and Se K-edge EXAFS (weighted by k^2) measured on polycrystalline FeSe (solid line) and the $K_{0.8}Fe_{1.6}Se_2$ crystal (open symbols) in the $E||ab$ geometry at $T=60$ K. Similar k -range (3.5 - 15.5 \AA^{-1}) is used to perform the FT for the comparison.

are expected to appear at ~ 3.0 - 4.5 \AA (upper panel). On the other hand, the Fe site nearest neighbours are Se (at a distance $\sim 2.4 \text{ \AA}$) and Fe (at a distance $\sim 2.7 \text{ \AA}$) in the $E||ab$ polarization (lower panel). The contribution of the Fe-Fe is not expected in the $E||c$ polarization and the main peak in the FT in this geometry should be merely due to Fe-Se bonds (middle panel). Contributions of Fe next near neighbours are expected to appear at longer distances ($R_{Fe-Fe}=3.91 \text{ \AA}$, $R_{Fe-K}=4.02 \text{ \AA}$ and $R_{Fe-Se}=4.62 \text{ \AA}$). Therefore, the main peak in the FT of the Fe K-edge EXAFS in the $E||ab$ geometry contains information on the Fe-Se and Fe-Fe bonds (lower panel) while the one in the $E||c$ have contribution only of Fe-Se bonds (middle panel), similar to the main FT peak of the Se K-edge EXAFS (upper panel). As a matter of fact, apart from the nearest neighbours, contribution expected from the farther atoms is apparently absent (or within the noise level). This is a characteristic feature of highly disordered systems and amorphous materials [29]. We will come back to discuss this, however, before that let us make a comparison between the local structure of FeSe and the $K_{0.8}Fe_{1.6}Se_2$.

Figure 2 compares Fourier transforms (FT) of the Fe and Se K-edge EXAFS signals ($T=60$ K) measured on the polycrystalline FeSe sample [8] and the $K_{0.8}Fe_{1.6}Se_2$ crystal in the $E||ab$ geometry. The Fe nearest neighbour in the FeSe are Se at a distance of ~ 2.4

Å and Fe atoms at a distance ~ 2.7 Å (two peak structure at ~ 1.5 - 3.0 Å), similar to the case of $K_{0.8}Fe_{1.6}Se_2$. Significantly intense features between 3-6 Å are due to longer Fe-Fe (~ 3.8 Å) and Fe-Se distances, and the multiple scatterings involving different near neighbours of the Fe atoms. Similarly, in the Se K-edge EXAFS of the FeSe we expect contribution from four Fe nearest neighbours at a distance ~ 2.4 Å (as in the $K_{0.8}Fe_{1.6}Se_2$). The next nearest neighbours are Se and Fe atoms and contributions of these distant shells clearly appear as a multiple structured peak at ~ 3.0 - 4.5 Å.

The comparison underlines significant differences in the local structure of the FeSe and the $K_{0.8}Fe_{1.6}Se_2$ systems. In particular, the FT of the $K_{0.8}Fe_{1.6}Se_2$ show only a single peak at ~ 2 Å that contains contribution from the Fe-Se distances (~ 2.4 Å) in the Se K-edge EXAFS and, Fe-Se and Fe-Fe contributions in the Fe K-edge EXAFS. The longer distances contributions are apparently absent in the $K_{0.8}Fe_{1.6}Se_2$ system. Also, the FT magnitude due to similar nearest neighbours is much weaker in the $K_{0.8}Fe_{1.6}Se_2$. In addition, the contribution from the Fe-Fe distances in the Fe K-edge EXAFS is strongly damped, indicating a large Fe site disorder. Apparently the EXAFS data reveal large overall local disorder in the $K_{0.8}Fe_{1.6}Se_2$ system, commonly seen in the local structure of amorphous systems [29]. On the other hand, the measured $K_{0.8}Fe_{1.6}Se_2$ sample is a very good single crystal, evident from sharp diffraction peaks [17], and such a large disorder in the local structure indicates that the system should be a some kind of glass.

Coming back, it is clear that only the nearest neighbours (i.e., Fe-Se and Fe-Fe bondlengths) contributions are visible in both Fe and Se K-edge EXAFS. Therefore our focus should be limited to these bondlengths. In the single-scattering approximation, the EXAFS amplitude is described by the following general equation [23]:

$$\chi(k) = \sum_i \frac{N_i S_0^2}{k R_i^2} f_i(k, R_i) e^{-\frac{2R_i}{\lambda}} e^{-2k^2 \sigma_i^2} \sin[2kR_i + \delta_i(k)] \quad (1)$$

where $N_i = 3 \cos^2 \theta_i$ is the number of neighbouring atoms at a distance R_i at an angle θ_i with respect to the x-ray beam polarization. S_0^2 is the passive electrons reduction factor, $f_i(k, R_i)$ is the backscattering amplitude, λ is the photoelectron mean free path, δ_i is the phase shift, and σ_i^2 is the correlated Debye-Waller factor (DWF) measuring the mean square relative displacements (MSRDs) of the photoabsorber-backscatterer pairs. EXCURVE 9.275 code (with calculated backscattering amplitudes and phase shift functions) is used for the EXAFS model fits [30]. Similar results were obtained with WINXAS package [31] in which the backscattering amplitudes and phase shifts were calculated using FEFF [32]. The E_0 , N_i and S_0^2 were fixed after a number of trials on different EXAFS scans with structural input from diffraction studies [17, 18, 19, 20, 33]. Only the radial distances R_i and the corresponding σ_i^2 , were allowed to vary in the least squares model fits for the temperature dependent study. A single shell (i.e., Fe-Se) was used to model the E||ab polarized Se K-edge EXAFS and E||c polarized Fe K-edge EXAFS. On the other hand, two shells (i.e., Fe-Se and Fe-Fe) were necessary to model the E||ab polarized Fe K-edge EXAFS. The number of independent data points, $N_{ind} \sim (2\Delta k \Delta R) / \pi$ [23] were about 17-18 ($\Delta k = 11$ - 12 Å⁻¹ and $\Delta R = 2.4$ Å), in the two

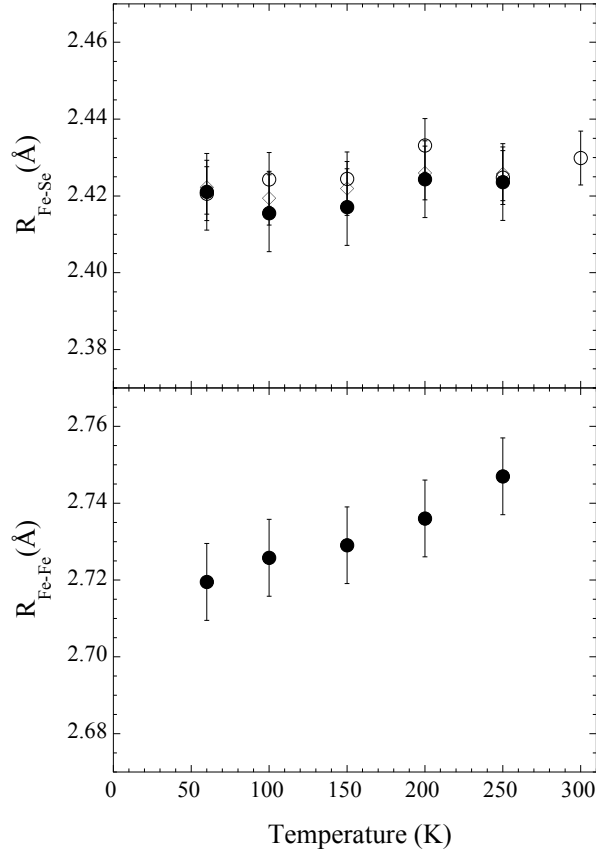


Figure 3. Fe-Se and Fe-Fe distances in the $K_{0.8}Fe_{1.6}Se_2$ as a function of temperature extracted from the polarized EXAFS spectra measured at Se and Fe K-edges. The Fe-Se bondlengths are similar irrespective of the selected absorbing atom and polarization, and slightly smaller than the average Fe-Se distance measured by diffraction. The open circles are from Se K-edge while the open diamonds represent the data from the E||c polarized Fe K-edge EXAFS. The closed circles are from the E||ab polarized Fe K-edge EXAFS. The error bars represent maximum uncertainty, determined using correlation maps between different parameters.

parameters (four parameters) fits for the E||ab Se K-edge and E||c Fe K-edge EXAFS (E||ab Fe K-edge EXAFS). The model fits are shown as insets to the Fig. 1.

Figure 3 shows temperature dependence of the local bondlengths determined by Fe K and Se K-edge EXAFS analysis. The Fe-Se distances determined by EXAFS data in different polarizations on two edges are similar within experimental uncertainties (upper panel). However, both Fe-Se and Fe-Fe distances (lower panel) appear slightly shorter than the average bondlengths determined by diffraction studies [17, 18, 19, 20, 33]. This may be due to largely disordered structure, as seen in the glasses [34, 35]. The Fe-Se bondlength hardly shows any change with temperature unlike the Fe-Fe distance (describing the in-plane lattice parameter) that varies with temperature showing relative flexibility of the later.

Figure 4 shows the correlated Debye Waller factors (σ^2), i.e., the MSRDS of the Fe-Se and the Fe-Fe pairs as a function of temperature for the $K_{0.8}Fe_{1.6}Se_2$, compared

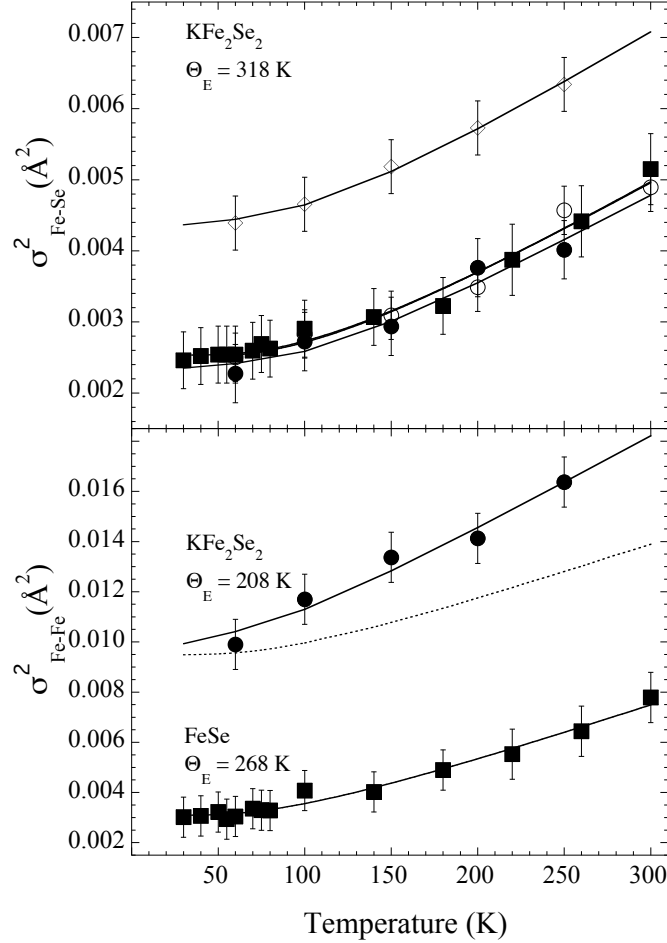


Figure 4. Temperature dependence of the Fe-Se and Fe-Fe MSRDs (symbols) for the $K_{0.8}Fe_{1.6}Se_2$ system determined by polarized EXAFS measured at Se and Fe K-edges. The empty (filled) circles are from E||ab polarized Se K-edge (Fe K-edge) EXAFS while the open diamonds represent the data from the E||c polarized Fe K-edge. The filled squares are the data obtained on the binary FeSe system [8]. The solid lines represent the correlated Einstein model fit to the data. The Einstein temperatures, θ_E , are ~ 318 K for the $K_{0.8}Fe_{1.6}Se_2$, similar to the Fe-Se bonds in the binary FeSe system (the maximum uncertainty is about ± 20 K). The σ_0^2 in the E||ab polarization is smaller (~ 0.0002) in compared to the one in the E||c (~ 0.002), consistent with large static disorder in the c-direction. While the θ_E for the Fe-Se remains similar to the binary FeSe system, the θ_E for the Fe-Fe is significantly different, suggesting large change in these bonds due to K-intercalation.

with the σ^2 of the two bondlengths for the binary FeSe system [8]. The σ^2 measured by EXAFS (represents distance broadening) is sum of temperature independent (σ_0^2) and temperature dependent terms, i.e. $\sigma^2 = \sigma_0^2 + \sigma^2(T)$. While the σ_0^2 (~ 0.0002) for the Fe-Se pairs in the E||ab polarization remains small (approximately similar to the case of the one in the binary FeSe), the σ_0^2 (~ 0.002) for the E||c is quite large. This merely indicates large disorder along the c-direction, likely to be due to the K-intercalation. Also, the σ_0^2 for the Fe-Fe is substantially large, a mere indicator of Fe site disorder.

On the other hand, temperature dependent $\sigma^2(T)$ is well described by the correlated Einstein model [23, 24], an appropriate approximation for local mode vibrations. The Einstein equation is given as:

$$\sigma^2(T) = \frac{\hbar^2}{2\mu k_B \theta_E} \coth \frac{\theta_E}{2T} \quad (2)$$

The Einstein temperature (θ_E , i.e., the Einstein frequency $\omega_E = k_B \theta_E / \hbar$) for the Fe-Se pairs remains similar to the one in the binary FeSe system ($\theta_E \sim 318$ K), indicating that local force constant ($k = \mu \omega_E^2$, where k is the effective force constant and μ is reduced mass of the Fe-Se pair) for the Fe-Se bonds is not very sensitive to the K- intercalation between the FeSe layers. The local force constant for Fe-Se bondlength is found to be $k \sim 5.8$ eV/Å², similar to the one in the binary FeSe superconductor. On the other hand, there is a substantial effect of intercalation on the Einstein temperature (local force constant) of the Fe-Fe pairs, estimated to be ~ 208 K ($k \sim 2.1$ eV/Å²) and ~ 268 K ($k \sim 3.5$ eV/Å²) respectively for the $K_{0.8}Fe_{1.6}Se_2$ and the binary FeSe. Therefore, it appears that the Fe-Fe bondlengths are relatively relaxed in the $K_{0.8}Fe_{1.6}Se_2$, consistent with a glassy nature of this system.

Considering the fact that the system is having a well defined crystal ordering, the glassy local structure could be due to freezing of iron vacancy order coupled with some other degrees of freedom. Several measurements have undelined that the magnetic ordering in this system co-exists with the superconductivity with a large iron moments ($3.3 \mu_B/Fe$) ordered antiferromagnetically along the c-axis [21, 22]. Present measurements reveal that there is; i) a large static disorder along the c-axis and ii) a large Fe-site disorder. In addition, the Fe-Fe network (in-plane lattice parameter) is relatively relaxed. Therefore it appears plausible to think that a frozen state of c-axis disorder (associated with local strain fields due to K-intercalation and iron vacancy order) coupled with magnetic order is realized. This results into a magnetic texture with large frozen magnetic moment and a relaxed Fe-Fe network. Thus, it is likely that the strain fields locally compress the FeSe-block and hence the T_c reaching to a value as high as 32 K, as it happens for FeSe under external pressure. Indeed, single-crystal x-ray diffraction has shown a clear evidence of nanoscale phase separation between a majority magnetic phase with iron vacancy ordering, co-existing with a minority compressed phase [17]. This situation is similar to granular superconductors in which a nanoscale superconducting phase coexisting in an insulating texture. Therefore, the physics of the $K_{0.8}Fe_{1.6}Se_2$ system should be quite similar to the physics of glasses and granular superconductors. It should be recalled that the thermodynamic and kinetic fragility of a glass is related to the number of potential energy minima in the phase space and the heights of the activation energy barriers separating these minima. The fact that the superconductivity in $K_{0.8}Fe_{1.6}Se_2$ system is strongly dependent on its thermal history [36], a characteristic feature of glasses, further underlines glassy nature of this system. The observation of glassy nature puts the system in the category of granular superconductors, consistent with the superconductivity in A15 systems [37] and recently observed fractal distribution enhanced superconductivity in superoxygenated La_2CuO_4

[38].

4. Summary

In summary, we have studied local structure of the superconducting $K_{0.8}Fe_{1.6}Se_2$ chalcogenide by polarized Fe and Se K-edges EXAFS. The EXAFS data provide a clear evidence of large local disorder in this system. Indeed the local structure of $K_{(0.8)}Fe_{(1.6)}Se_2$ is similar to that of the amorphous materials indicating glassy nature of the system. The local bondlengths are found to be slightly shorter than the average diffraction distances, a characteristic feature of glasses. The mean square relative displacements (MSRD) of Fe-Se and Fe-Fe bondlengths are well described by the correlated-Einstein model with similar Einstein-temperatures in all the polarizations, albeit the stastic component along the c-axis is much larger, likely to be due to substitutional disorder in the K layer. While the Fe-Se bondlengths remains highly covalent in the $K_{0.8}Fe_{1.6}Se_2$, similar to the one found in the binary FeSe superconductor, the Fe-Fe bondlength is characterized by much smaller force constant compared to the binary FeSe. Such a local relaxation of the Fe-Fe bondlength results in a compression of the FeSe unit, as happens under external pressure, and hence the superconductivity at high T_c in the title system should be due to locally compressed nanoscale minority phase, coexisting with the normal magnetic phase, similar to the case of granular superconductors.

Note added: After finishing this manuscript we came across a very recent publication by Tyson *et al* [39] reporting similar kind of measurements on the $K_{0.8}Fe_{1.6+x}Se_2$ system finding a large disorder, similar to the one reported in this manuscript. However, Tyson *et al* have compared the data with the one obtained on 1111-iron pnictide unlike the present study in which a direct comparison with the binary FeSe has allowed us to clearly identify the effect on the local structure due to K-intercalation. Therefore, the glassy nature revealed in these measurements should provide further insight to our understanding of these superconductors.

Acknowledgments

The authors wishes to thank ESRF staff for the help and support during the experimental runs.

References

- [1] Y. Kamihara, T. Watanabe, M. Hirano and H. Hosono, J. Am. Chem. Soc. 130, 3296 (2008).
- [2] D.C. Johnston, Advances in Physics 59, 803 (2010).
- [3] Y. Mizuguchi, Y. Takano, J. Phys. Soc. Jpn. 79, 102001 (2010).
- [4] A. Iadecola, S. Agrestini, M. Filippi, L. Simonelli, M. Fratini, B. Joseph, D. Mahajan and N. L. Saini, Europhysics Letters 87, 26005 (2009).
- [5] B. Joseph, A. Iadecola, M. Fratini, A. Bianconi, A. Marcelli and N.L. Saini, Journal of Physics: Condensed Matter 21, 432201 (2009); W. Xu, A. Marcelli, B. Joseph, A. Iadecola, W. S. Chu, D. Di Gioacchino, A. Bianconi, Z. Y. Wu, and N. L. Saini, Journal of Physics: Condensed Matter

- 22, 125701 (2010); W. Xu, B. Joseph, A. Iadecola, A. Marcelli, W. S. Chu, D. Di Gioacchino, A. Bianconi, Z. Y. Wu and N. L. Saini, EPL 90, 57001 (2010).
- [6] Y. Mizuguchi, F. Tomioka, S. Tsuda, T. Yamaguchi, and Y. Takano, Appl. Phys. Lett. 93, 152505 (2008).
- [7] S. Medvedev, T. M. McQueen, I. A. Troyan, T. Palasyuk, M. I. Erements, R. J. Cava, S. Naghavi, F. Casper, V. Ksenofontov, G. Wortmann and C. Felser, Nature Materials 8, 630 - 633 (2009).
- [8] B. Joseph, A. Iadecola, A. Puri, L. Simonelli, Y. Mizuguchi, Y. Takano, and N. L. Saini, Phys. Rev. B 82, 020502(R) (2010); A. Iadecola, B. Joseph, L. Simonelli, Y. Mizuguchi, Y. Takano and N. L. Saini, EPL 90, 67008 (2010); A. Iadecola, B. Joseph, A. Puri, L. Simonelli, Y. Mizuguchi, D. Testemale, O. Proux, J-L. Hazemann, Y. Takano and N L Saini, Journal of Physics: Condensed Matter 23, 425701 (2011).
- [9] J. Guo, S. Jin, G. Wang, S. Wang, K. Zhu, T. Zhou, M. He and X. Chen, Phys. Rev. B 82, 180520 (2010).
- [10] A. F. Wang, J. J. Ying, Y. J. Yan, R. H. Liu, X. G. Luo, Z. Y. Li, X. F. Wang, M. Zhang, G. J. Ye, P. Cheng, Z. J. Xiang, and X. H. Chen, Phys. Rev. B 83, 060512(R) (2011).
- [11] Chun-Hong Li, Bing Shen, Fei Han, Xiyu Zhu, Hai-Hu Wen, Phys. Rev. B 83, 184521 (2011).
- [12] Minghu Fang, Hangdong Wang, Chiheng Dong, Zujuan Li, Chunmu Feng, Jian Chen, H. Q. Yuan, EPL, 94 27009 (2011).
- [13] J. J. Ying, X. F. Wang, X. G. Luo, A. F. Wang, M. Zhang, Y. J. Yan, Z. J. Xiang, R. H. Liu, P. Cheng, G. J. Ye, X. H. Chen, Phys. Rev. B 83, 212502 (2011).
- [14] Lin Zhao, Daixiang Mou, Shanyu Liu, Xiaowen Jia, Junfeng He, Yingying Peng, Li Yu, Xu Liu, Guodong Liu, Shaolong He, Xiaoli Dong, Jun Zhang, J. B. He, D. M. Wang, G. F. Chen, J. G. Guo, X. L. Chen, Xiaoyang Wang, Qinjun Peng, Zhimin Wang, Shenjin Zhang, Feng Yang, Zuyan Xu, Chuangtian Chen, and X. J. Zhou, Phys. Rev. B 83, 140508 (2011).
- [15] T. Qian, X.-P. Wang, W.-C. Jin, P. Zhang, P. Richard, G. Xu, X. Dai, Z. Fang, J.-G. Guo, X.-L. Chen, and H. Ding, Phys. Rev. Lett. 106, 187001 (2011).
- [16] I. Mazin, Physics 4, 26 (2011).
- [17] A. Ricci, N. Poccia, B. Joseph, G. Arrighetti, L. Barba, J. Plaisier, G. Campi, Y. Mizuguchi, H. Takeya, Y. Takano, N.L. Saini and A. Bianconi, Supercond. Sci. Technol. 24 082002, (2011); A. Ricci, N. Poccia, G. Campi, B. Joseph, G. Arrighetti, L. Barba, M. Reynolds, M. Burghammer, H. Takeya, Y. Mizuguchi, Y. Takano, M. Colapietro, N. L. Saini, and A. Bianconi, Phys. Rev. B 84, 060511(R) (2011).
- [18] F. Ye, S. Chi, Wei Bao, X. F. Wang, J. J. Ying, X. H. Chen, H. D. Wang, C. H. Dong, and Minghu Fang, Phys. Rev. Lett. 107, 137003 (2011).
- [19] P. Zavalij, Wei Bao, X. F. Wang, J. J. Ying, X. H. Chen, D. M. Wang, J. B. He, X. Q. Wang, G. F. Chen, P.-Y. Hsieh, Q. Huang, and M. A. Green, Phys. Rev. B 83, 132509 (2011).
- [20] Z. Wang, Y. J. Song, H. L. Shi, Z. W. Wang, Z. Chen, H. F. Tian, G. F. Chen, J. G. Guo, H. X. Yang, and J. Q. Li, Phys. Rev. B 83, 140505 (2011).
- [21] Wei Bao, Q. Huang, G. F. Chen, M. A. Green, D. M. Wang, J. B. He, X. Q. Wang, Y. Qiu, Chinese Phys. Lett. 28, 086104 (2011).
- [22] V. Yu. Pomjakushin, D. V. Sheptyakov, E. V. Pomjakushina, A. Krzton-Maziopa, K. Conder, D. Chernyshov, V. Svitlyk, Z. Shermadini Phys. Rev. B 83, 144410 (2011); V. Yu Pomjakushin, E. V. Pomjakushina, A. Krzton-Maziopa, K. Conder and Z. Shermadini, J. Phys.: Condens. Matter 23, 156003 (2011).
- [23] X-ray Absorption: Principles, Applications, Techniques of EXAFS, SEXAFS, XANES, edited by R. Prins and D. C. Koningsberger (Wiley, New York, 1988).
- [24] A. Bianconi and N.L. Saini, Structure and Bonding 114, 287 (2005); N. L. Saini, A. Lanzara, H. Oyanagi, H. Yamaguchi, K. Oka, T. Ito, and A. Bianconi, Physical Review B 55, 12759 (1997); N. L. Saini, A. Bianconi, and H. Oyanagi, Journal of the Physical Society of Japan 70, 2092 (2001).
- [25] C. J. Zhang, H. Oyanagi, Z. H. Sun, Y. Kamihara, and H. Hosono, Phys. Rev. B 81, 094516 (2010).
- [26] B. Joseph, A. Iadecola, L. Malavasi and N. L. Saini, J. Phys.: Condens. Matter 23, 265701 (2011).

- [27] Y. Mizuguchi, H. Takeya, Y. Kawasaki, T. Ozaki, S. Tsuda, T. Yamaguchi, and Y. Takano, *Appl. Phys. Lett.* 98, 042511 (2011).
- [28] L. Troger, D. Arvanitis, K. Baberschke, H. Michaelis, U. Grimm, and E. Zschech, *Phys. Rev. B* 46, 3283 (1992).
- [29] see, e.g., a recent review on glasses by G. N. Greaves and S. Sen, *Adv. in Phys.* 56, 1 (2007) and relevant references.
- [30] S.J. Gurman, *J. Synch. Rad.* 2, 56-63 (1995).
- [31] T. Ressler, *Journal of Synchrotron Radiation* 5, 118 (1998).
- [32] J. Mustre de Leon, J. J. Rehr, S. I. Zabinsky, R. C. Albers, *Phys. Rev. B* 44, 4146 (1991); J.J. Rehr and R.C. Albers, *Rev. Mod. Phys.* 72, 621 (2000).
- [33] J. Bacsá, A. Y. Ganin, Y. Takabayashi, K. E. Christensen, K. Prassides, M. J. Rosseinsky and J. B. Claridge, *Chem. Sci.* 2, 1054 (2011).
- [34] A. V. Kolobov, H. Oyanagi, K. Tanaka, and Ke. Tanaka, *Phys. Rev. B* 55, 726 (1997); A. V. Kolobov, H. Oyanagi, and K. Tanaka, *Phys. Rev. Lett.* 87, 145502 (2001).
- [35] M. Majid, S. Benazeth, C. Souleau, and J. Purans, *Phys. Rev. B* 58, 6104 (1998).
- [36] Fei Han, Bing Shen, Zhen-Yu Wang, Hai-Hu Wen, arXiv:1103.1347v1.
- [37] L. R. Testardi, *Rev. Mod. Phys.* 47, 637 (1975).
- [38] M. Fratini, N. Poccia, A. Ricci, G. Campi, M. Burghammer, G. Aeppli, and A. Bianconi, *Nature (London)* 466, 841 (2010).
- [39] T. A. Tyson, T. Yu, S. J. Han, M. Croft, G. D. Gu, I. K. Dimitrov, and Q. Li, *Phys. Rev. B* 85, 024504 (2012).